

*Research article***Light-soaking tests of zinc oxide photoanodes sensitized with an indoline dye on different transparent conductive substrates****B. Onwona-Agyeman<sup>1</sup>, A. Yaya<sup>1,\*</sup>, G. R. A. Kumara<sup>2</sup> and M. Nakao<sup>3</sup>**<sup>1</sup> Department of Materials Science and Engineering, School of Engineering Sciences, University of Ghana, Legon, Ghana<sup>2</sup> Institute of Fundamental Studies, Hantana Road, Kandy, Sri Lanka<sup>3</sup> Department of Basic Sciences, Kyushu Institute of Technology, Kitakyushu, Japan\* **Correspondence:** Email: [ayaya@ug.edu.gh](mailto:ayaya@ug.edu.gh).

**Abstract:** Dye-sensitized solar cells (DSCs) were prepared using porous zinc oxide (ZnO) films on aluminum-doped zinc oxide (AZO) and fluorine-doped tin oxide (FTO) transparent conductive glass substrates. X-ray diffraction measurements revealed that, the porous ZnO films were crystallographically oriented differently on the two transparent substrates. The two DSCs were prepared using metal-free indoline dye as the sensitizer and a liquid electrolyte as the hole conductor. Measurements of the power conversion efficiency of the two DSCs over a period of time showed deterioration in the conversion efficiency of the DSCs with the deterioration being faster in ZnO/FTO than ZnO/AZO. The deterioration is attributed mainly to the decrease in light-harvesting ability of the sensitizer and recombination of photo-excited electrons resulting in the decrease in the short-circuit photocurrent densities and the open-circuit voltages in both DSCs during the light-soaking process.

**Keywords:** crystallographic orientation; photovoltaic; transparent conductor; thin film; spray deposition; semiconductor

---

**1. Introduction**

Photovoltaic energy conversion is the direct production of electrical energy from the electromagnetic radiation (solar spectrum) by solar cells. The basic mechanisms needed in a solar cell to convert sunlight to electricity are; the absorption of photons, separation of the photons into

charges, transporting the photogenerated charges and finally extracting the charges at the contact points. There is a material responsible for each process and the performance of each material greatly affects the overall performance of the solar cell device. The dye-sensitized solar cell (DSC) is a photovoltaic cell first developed by O'Reagan and Grätzel in 1991 [1] and recently a tandem-type DSC has been developed using two types of dyes [2]. The DSC is made up of a transparent n-type semiconductor as an electrode on which a porous wide bandgap semiconductor is deposited. The surface area of this porous semiconductor is designed to be large, in order to accommodate monolayer of dye on its surface. The dye sensitizer is the absorber of sunlight in the DSC. A platinum-coated (Pt) glass is then employed as a counter electrode in such a way that the dye-coated porous semiconductor is sandwiched between the transparent semiconductor and the counter electrode. An electrolyte is then used to permeate the dye-coated porous semiconductor network to establish an electrical contact between the dye and the counter electrode. The conversion of sunlight-to-electric power in DSC begins with the absorption of sunlight (photons) by the dye and the dissociation of photons at the dye-semiconductor interface [2]. The photogenerated electrons are then injected into the conduction band of the porous structured semiconductor where they are transported through the mesoporous network to the transparent electrode. The liquid electrolyte is the pathway for the holes from the oxidized dye to be transported back to the Pt electrode [3].

Ruthenium-based complex dyes were initially used as sensitizers in DSCs [4–7] but now several metal-free dyes [8–14] and inorganic quantum dots [15,16] have been employed as sensitizers. The metal-free organic dye complexes have certain advantages over the metal-based complex dyes such as easier synthesizing route and are relatively cheaper because they do not contain any rare metal. A major setback of metal-free dyes is their stability. A long life span and stability of DSC are critical parameters for the realization of large-scale practical devices. An important component in the DSC is the transparent electrode where the photogenerated electrons travelling through the mesoporous semiconductor are collected into the external circuit. The transparent electrode, an n-type oxide semiconductor, also known as transparent conducting oxide (TCO) must be optically transparent for sunlight to enter the DSC and also must be electrically conductive. Therefore, the interface between the TCO and the porous semiconductor plays a crucial role during the process of converting sunlight to electricity. Initially, anatase  $\text{TiO}_2$  was used as the porous semiconductor but other wide band semiconductors such as  $\text{SnO}_2$  and  $\text{ZnO}$  have been utilized [12,17,18]. Currently, the power conversion efficiency of  $\text{TiO}_2$ -based DSCs are higher than that of the corresponding  $\text{ZnO}$  and  $\text{SnO}_2$  DSCs. The DSC is fabricated by depositing the porous semiconductor onto the TCO and heating at  $500\text{ }^\circ\text{C}$  for 30 min. This thermal treatment is important in order to create electrical contact between particles within the mesoporous network to facilitate the flow of photogenerated electrons. If the TCO and the porous semiconductor materials are different, lattice mismatch and difference in thermal expansion coefficient will create defects at the interface thereby slowing down or trapping of photogenerated electrons from the porous semiconductor to the TCO. These processes affect the conversion efficiency and the stability of DSC.

In this work, we have used two different TCOs, an aluminum-doped zinc oxide thin film (AZO) which was prepared by radio frequency (rf) magnetron sputtering and a commercially available fluorine-doped tin oxide (FTO) to fabricate porous  $\text{ZnO}$  DSC sensitized with a metal-free indoline dye. The TCOs (AZO and FTO) used were characterized by a Scanning Electron Microscope (SEM), X-ray diffractometer (XRD) and a UV-visible spectrophotometer to study the surface morphology, film structure and orientation and optical transmission of the films.

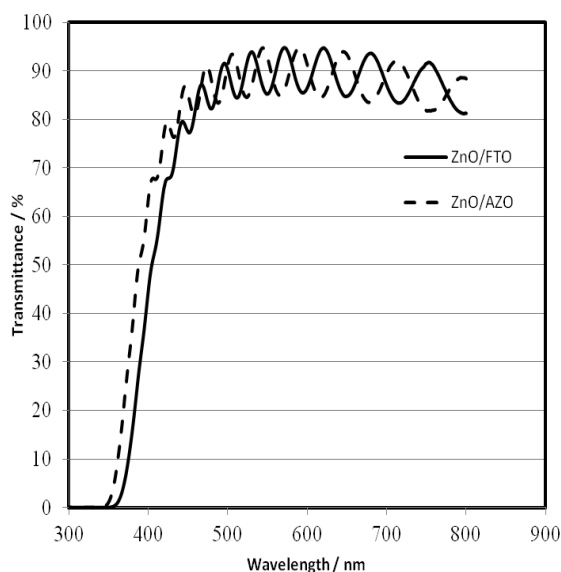
## 2. Experimental

The AZO films were prepared by rf magnetron sputtering technique with a commercially available ZnO target doped with alumina ( $\text{Al}_2\text{O}_3$  2.5 wt. %). During the deposition, the sputtering pressure was maintained at 3 Pa, substrate temperature at 300 °C and rf power of 100 W. The crystal structure and orientation of the AZO and FTO films were studied by X-ray diffraction (XRD, JEOL JDX-3500K) using filtered copper  $K\alpha$  ( $\lambda = 0.15418$  nm) in a scan mode and the optical transmission spectra were measured using UV/Visible spectrophotometer (JASCO V560) and all the transmission spectra data were taken at room temperature in air, with average transmittance within the wavelength range of 400–800 nm. The surface morphologies of the AZO and FTO were observed with Field Emission Scanning Electron Microscope (FE-SEM; JEOL JSM-700).

Porous ZnO films were deposited on the AZO and FTO coated glass substrates by mixing 0.6 g of ZnO powder (average particle size ~20 nm), few drops of glacial acetic acid and ethanol (40 ml) and ultrasonically dispersing the solution for 10 min. The mixture was then sprayed onto the heated (150 °C) AZO and FTO substrates using a spray gun yielding a film thickness of about 6  $\mu\text{m}$  and subsequently sintering in air at 500 °C for 30 min. The ZnO photoelectrodes (active surface area 0.25  $\text{cm}^2$ ) were then immersed in a mixture of acetonitrile and *tert*-butanol (volume 1:1) containing  $5 \times 10^{-4}$  M indoline dye D-358 (Mitsubishi Paper Mills) for 10 hrs. The dye-coated ZnO photoelectrodes were removed, rinsed with acetonitrile and allowed to dry in air. Construction of the DSCs were carried out by sandwiching the dye-coated ZnO electrode with a sputtered platinum film counter electrode and the intervening space filled with a liquid electrolyte (electrolyte composition: 0.1 M LiI, 0.05 M  $\text{I}_2$ , 0.6 M dimethylpropyl-imidazolium iodide in methoxyacetonitrile). The conversion efficiency stability tests were carried out by measuring the current-voltage (I-V) characteristics of the two DSCs at an interval of 5 min at AM 1.5 (1000  $\text{W m}^{-2}$ ) simulated sunlight irradiation using a calibrated solar cell evaluation system (PECell-PEC L-12, Japan).

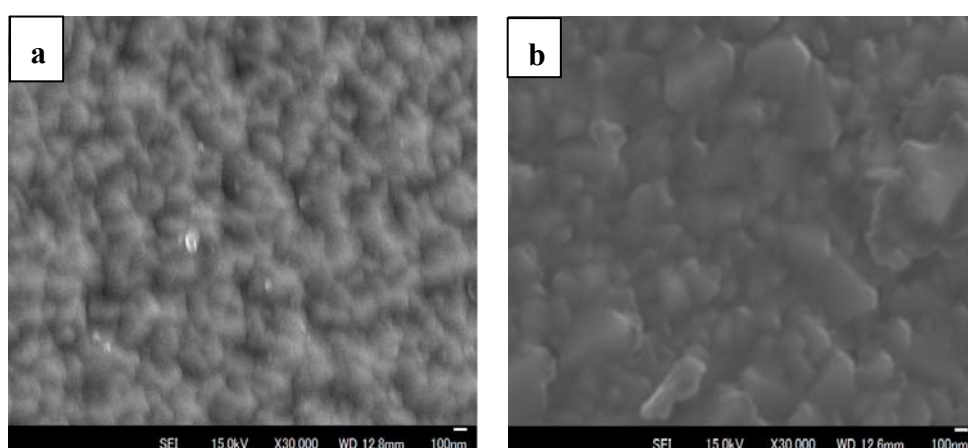
## 3. Results and discussion

Figure 1 shows the optical transmittance spectra of the sputtered AZO and the commercially available FTO films in the wavelength range between 400 and 800 nm. The average transmittances of the two films were above 80% and the oscillatory character of the curves is due to interference effects [19]. In general, for a film to be used as a TCO in a solar cell, the average transmittance must be more than 80% for significant amount of sunlight to be admitted into the device. The two substrates are therefore suitable to be used as transparent electrodes in the DSC.



**Figure 1.** Transmittance spectra for AZO and FTO thin films before the deposition of porous ZnO film.

The surface morphologies of AZO and FTO films were observed using an FE-SEM and the images are shown in Figure 2. The surface properties of the TCOs are very crucial as the porous semiconductor is deposited directly onto it. Again, photoelectrons injected into the conduction band, are transported through the interface to the TCO for collection into the external circuit. Therefore, if there is/are any significant morphological differences between the surface of the TCO and that of the porous semiconductor, photoelectrons may be trapped or prevented from reaching the external circuit. From Figure 2, there are clear morphological differences between the AZO and FTO surfaces used in this work. Therefore, changes observed in the surface morphologies of the AZO and FTO will affect electron transfer from the porous ZnO film.



**Figure 2.** Surface morphologies of (a) AZO, and (b) FTO transparent films before the deposition of porous ZnO.

The X-ray diffraction patterns of the porous ZnO films on the AZO and FTO coated glass substrates are shown in Figure 3. The porous ZnO films on the two transparent substrates are polycrystalline in nature with well defined diffraction peaks. The ZnO film prepared on the AZO substrate exhibit high peak intensity along the (002) direction as required for opto-electronic applications such as in solar cells [20,21]. On the other hand, the (002) diffraction peak was highly suppressed when the ZnO was prepared on the FTO. The change in the crystallographic orientation of the planes within the ZnO film when deposited on AZO and FTO is very interesting as it will affect electron movement to the TCOs when they are in contact in an opto-electronic device such as DSC. The dominant (002) peak in the XRD pattern of the ZnO when deposited on AZO indicates that, electron can travel with ease to the AZO/TCO because majority of the grains in the ZnO are oriented along the (002) plane with relatively few grain boundary defects. But the suppression of the (002) peak and the appearance and dominance of the (100) and (101) peaks when the ZnO is deposited on the FTO implies more grain boundary defects and therefore electron movement within the porous ZnO will be restricted. Figure 4 is the structural formula of the D358 indoline dye used in sensitizing the two DSCs. The indoline sensitizers are metal-free organic complex structures and relatively cheaper than the metal-based complex dyes and also have higher extinction coefficients [13].

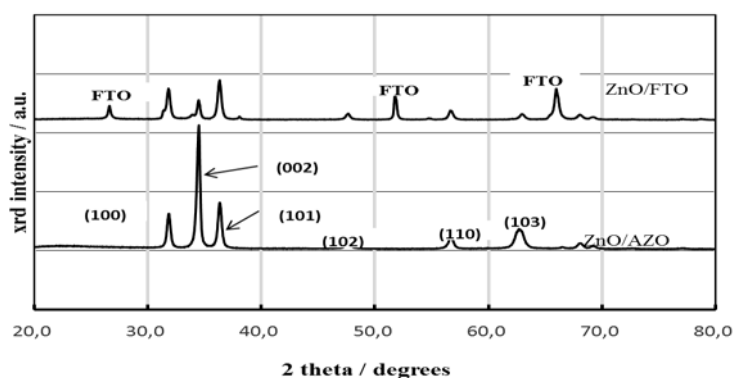


**Figure 3.** XRD patterns of porous ZnO films sprayed onto heated AZO and FTO substrates at 150 °C.

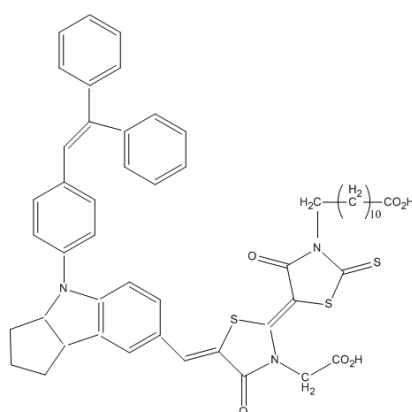


**Figure 4.** Structural formular of the indoline dye D358 used in the sensitization of the ZnO DSC.

Tables 1 and 2 summarize the  $I$ - $V$  parameters of the ZnO/AZO and ZnO/FTO DSCs sensitized with the indoline dye using a calibrated solar cell simulator under AM 1.5 ( $1000 \text{ W m}^{-2}$ ) simulated sunlight. Both the short-circuit photocurrent density ( $J_{sc}$ ) and the open-circuit voltage decreases with time. These two  $I$ - $V$  parameters strongly affect the overall conversion efficiency of a solar cell. The decrease in intensity of the  $J_{sc}$  with time is attributed to the poor light harvesting ability of the indoline dye and the decrease of the  $V_{oc}$  is also due to the recombination of photoelectrons that are suppose to travel through the mesoporous ZnO film to the external circuit. The metal-free organic dye sensitizer used in this work is suppose to harvest significant amount of photons (light) consistently over long period of time. An important question for the practical realization of these mesoscopic solar cells concerns the stability of these devices under prolonged exposure to solar radiation. The initial conversion efficiencies of the two solar cells were similar (5.01% and 5.07% for ZnO/AZO and ZnO/FTO respectively) but after 45 min of light soaking the conversion efficiency of both solar cells decreased to 2.46% and 2.09% respectively. Figures 5 and 6 shows the  $I$ - $V$  characteristics of the ZnO/AZO and ZnO/FTO DSCs for the as-measured and after 45 min light-soaking. The electrolyte is a key component in this type of solar cell and is responsible for the collection of holes from the cathode and transporting them back to the dye. The electrolyte used in this work is the iodide/triiodide ( $\text{I}^-/\text{I}_3^-$ ) and it works well because of its kinetics within the DSC [21].

**Table 1.**  $I$ - $V$  parameters ( $J_{sc}$  = short-circuit photocurrent density,  $V_{oc}$  = open-circuit voltage, FF = Fill factor and  $\eta$  = efficiency) of ZnO/AZO DSC measured under simulated sunlight for 45 min.

min	$V_{oc}$ (mV)	$J_{sc}$ (mA/cm <sup>2</sup> )	FF	$\eta$ (%)
0	670	12.77	0.59	5.07
5	668	11.18	0.64	4.79
10	671	10.45	0.65	4.58
15	670	9.27	0.67	4.15
20	637	9.35	0.62	3.70
25	628	8.28	0.64	3.33
30	624	8.03	0.62	3.09
35	623	6.90	0.64	2.74
40	631	6.27	0.66	2.62
45	620	5.89	0.68	2.46

**Table 2.**  $I$ - $V$  parameters ( $J_{sc}$  = short-circuit photocurrent density,  $V_{oc}$  = open-circuit voltage, FF = Fill factor and  $\eta$  = efficiency) of ZnO/FTO DSC measured under simulated sunlight for 45 min.

min	$V_{oc}$ (mV)	$J_{sc}$ (mA/cm <sup>2</sup> )	FF	$\eta$ (%)
0	647	12.73	0.62	5.10
5	659	11.21	0.64	4.69
10	623	11.16	0.65	4.49
15	616	10.99	0.64	4.31
20	614	10.04	0.65	4.00

*Continued on next page*

min	Voc (mV)	Jsc (mA/cm <sup>2</sup> )	FF	η (%)
25	612	9.34	0.64	3.67
30	610	7.99	0.65	3.16
35	595	6.93	0.65	2.68
40	587	6.00	0.67	2.35
45	588	5.20	0.68	2.09

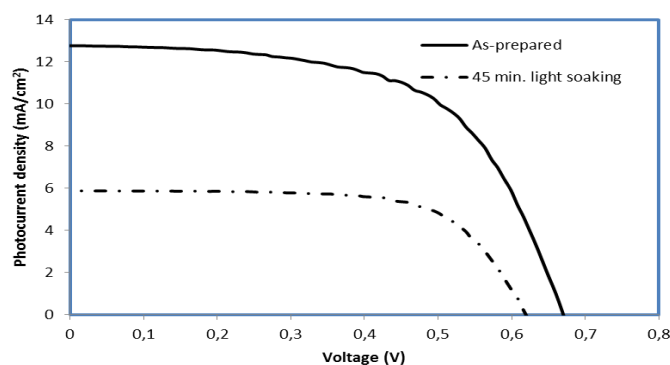


**Figure 5.** *I-V* characteristics of ZnO/AZO DSC under simulated sunlight; as-prepared and after 45 min light soaking.

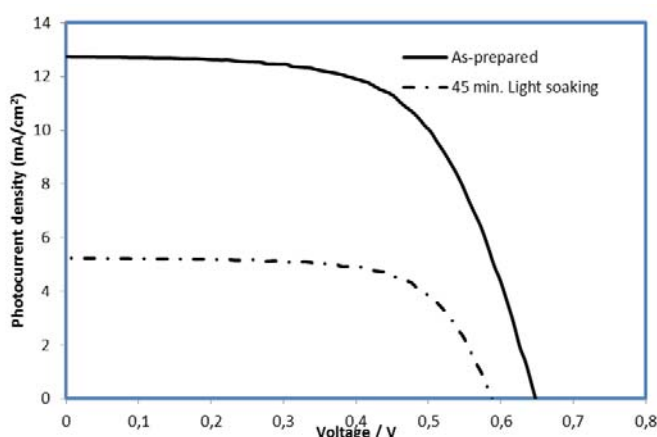


**Figure 6.** *I-V* characteristics for ZnO/FTO DSC; as-prepared and after 45 min light-soaking.

The rapid deterioration in efficiency of the ZnO/FTO with respect to that of ZnO/AZO shows the potential of AZO film as TCO; which is cheaper than FTO and tin-doped indium oxide TCOs. The surface morphologies of the two TCOs as shown in Figure 2 illustrate different surface features and may be responsible for the observed different growth direction of the porous ZnO on the surface of the AZO and FTO. In a DSC, after injection of photo-excited electrons from the Lowest Unoccupied Molecular Orbital (LUMO) of the dye to the conduction band of the semiconductor, the electrons are expected to travel through the mesoporous network of the semiconductor to the underlying TCO. If the porous semiconductor is made of different grain boundaries (such as porous structures having different oriented X-ray peaks) it is difficult for electrons to travel through such a network. The grain boundaries are made up of traps, defects and other structures that impede the

electron movement. During the construction of DSCs, the photoanode (TCO and porous semiconductor) is heated to about 500 °C to eliminate traces of organic components in the porous semiconductor and also to create electrical pathways for the movement of the photo-injected electrons. This heat treatment can cause the formation of defects in the interface if the TCO and the porous oxide semiconductor are made of different materials as a result of thermal expansion differences. Clearly, the ZnO on the FTO exhibited similar features such as mixed XRD peak orientations resulting in films with grain boundaries. Long-term stability tests of large-area DSC using mesoporous TiO<sub>2</sub> sensitized with ruthenium-based complex dyes have been studied [23,25]. It is therefore important to look at the stability of these metal-free dyes as attempts are being made to improve their conversion efficiencies. For an ideal sensitizer, it should be stable to endure long exposure to sunlight without significant degradation. The LUMO level of the D358 dye used in this work is higher than the conduction band of the ZnO and its HOMO level is sufficiently low to accept holes from the electrolyte [13]. The most important parameters in the evaluation of performance of a solar cell are the open circuit voltage  $V_{oc}$ , the short circuit current  $I_{sc}$  and the fill factor  $FF$ . Since the cell efficiency is proportional to the product of these three parameters, the optimization of a solar cell can be attained by increasing any of these. While  $I_{sc}$  can be related to the total absorption of the electromagnetic radiation,  $V_{oc}$  depends on recombination losses, but a clear connection between  $FF$  and properties like mobility, contact properties and recombination constants is more difficult to establish and therefore still a subject of discussion, in particular for organic based devices such as DSC [26].

In our work, both the  $I_{sc}$  and  $V_{oc}$  decreased after 45 min of light exposure but the  $FF$  increased. From the above, the continuous exposure of the solar cell may have improved certain properties such as mobility of the photogenerated charges, improved the contact properties of both electrodes, etc. Since the  $V_{oc}$  and  $I_{sc}$  decreased consistently with exposure time, the increase in  $FF$  could not affect the resultant conversion efficiency. More work needs to be done to understand this occurrence.

From the  $I$ - $V$  parameters obtained, the two DSCs clearly show that this indoline dye could not withstand prolong exposure to sunlight and therefore further development is required to improve its light-soaking stability. From this study, it is clear that AZO can be used effectively as TCO in future DSCs in attempts to commercialize these low-cost mesoscopic solar cells.

#### 4. Conclusions

We have prepared two porous ZnO-based dye-sensitized solar cells with different TCOs; an aluminum-doped ZnO and fluorine-doped SnO<sub>2</sub> and sensitized them with an indoline dye. We have subjected these two DSCs to light-soaking test for 45 min and measured their solar-to-electric power conversion efficiency at 5 min interval over 45 min. The conversion efficiency in both DSCs decreased with time and that was attributed to the degradation of the sensitizer which affected the short-circuit photocurrent and the open-circuit voltage. We also found that, the ZnO/FTO DSC showed rapid deterioration in conversion efficiency than ZnO/AZO and the rapid deterioration was attributed to several factors including changes in crystallographic orientation, thermal expansion difference, lattice constants mismatch between the porous ZnO and transparent conductive FTO substrate.



## Conflict of interest

The Authors declare no conflict of interest or whatsoever to this publication.

## References

1. O'Regan B, Grätzel M (1991) A low cost, high-efficiency solar cell based on dye-sensitized colloidal TiO<sub>2</sub> films. *Nature* 353: 737–740.
2. Ali AK, Eli SE, Hassoon KI, et al. (2018) Design of high-efficiency tandem dye-sensitized solar cell with two-photoanodes toward the broader light harvesting. *Dig J Nanomat Biostructures* 13: 299–305.
3. Grätzel M (2004) Conversion of sunlight to electric power by nanocrystalline dye-sensitized solar cell. *J Photoch Photobio A* 164: 3–14.
4. Denizalti S, Ali AK, Ela C (2018) Mesut Ekmekci, Sule Erten-Ela, Dye-sensitized solar cells using ionic liquids as redox mediator. *Chem Phys Lett* 691: 373.
5. Chiba Y, Islam A, Watanabe Y, et al. (2006) Dye-sensitized solar cells with conversion efficiency of 11.1%. *Jpn J Appl Phys* 45: L638–L640.
6. And AK, Gratzel M (2002) Dye-sensitized Core-shell Nanocrystals: Improved Efficiency of Mesoporous Tin Oxide electrodes Coated with Thin Layer of an insulating Oxide. *Chem Mater* 14: 2930–2935.
7. Zaban A, Chen SG, Chappel S, et al. (2000) Bilayer nanoporous electrodes for dye-sensitized solar cell. *Chem Commun* 22: 2231–2232.
8. Tennakone K, Bandaranayake PKM, Jayaweera PVV, et al. (2002) Dye-sensitized composite semiconductor nanostructures. *Physica E* 14: 190–196.
9. Onwona-Agyeman B, Nakao M, Kohno T, et al. (2013) Preparation and characterization of sputtered aluminium and gallium Co-doped ZnO films as conductive substrates in dye-sensitized solar cells. *Chem Eng J* 219: 273–277.
10. Ileperuma OA, Kumara GRA, Murakami K (2008) Quasi-solid polymer electrolytes based on polyacrylonitrile and plasticizers for indoline dye-sensitized solar cells of efficiency 5.3%. *Chem Lett* 37: 36–37.
11. Onwona-Agyeman B, Nakao M, Kumara GRA (2010) Photoelectrochemical solar cells made from SnO<sub>2</sub>/ZnO films sensitized with an indoline dye. *J Mater Res* 25: 1838.
12. Konno A, Kumara GRA, Kaneko S, et al. (2007) Solid-state solar cells sensitized with indoline dye. *Chem Lett* 36: 716–717.
13. Onwona-Agyeman B, Kaneko S, Kumara A, et al. (2005) Sensitization of Nanocrystalline SnO<sub>2</sub> films with indoline dyes, *Jpn J Appl Phys* 44: L731–L733.
14. Horiuchi T, Miura H, Uchida S (2003) High-efficient Metal-free organic dyes for dye-sensitized solar cells. *Chem Commun* 35: 3036–3037.
15. Li SL, Jiang KJ, Shao KF, et al. (2006) Novel organic dyes for efficient dye-sensitized solar cells. *Chem Commun* 37: 2792–2794.
16. Zaban A, Micic OI, Gregg BA, et al. (1998) Photosensitization of nanoporous TiO<sub>2</sub> electrodes with InP quantum dots. *Langmuir* 14: 3153–3156.

17. Shen Q, Arae D, Toyoda T (2004) Photosensitization of nanostructured TiO<sub>2</sub> with CdSe quantum dots: Effects of microstructure and electron transport in TiO<sub>2</sub> substrates. *J Photoch Photobio A* 164: 75–80.
18. Onwona-Agyeman B, Nakao M, Kumara GRA, et al. (2014) Sensitization of zinc oxide photoanode with an indoline dye. *Prog Photovoltaics Res Appl* 22: 661–665.
19. Onwona-Agyeman B, Nakao M, Kitaoka T (2014) Photovoltaic performance of spray-coated zinc oxide nanoparticles sensitized with metal-free indoline dyes. *J Mat Sci Res* 3: 87.
20. Nanto H, Minami T, Shoji S, et al. (1984) Electrical and optical properties of zinc oxide films prepared by rf magnetron sputtering for transparent electrode applications. *J Appl Phys* 55: 1029.
21. Xu WZ, Ye ZZ, Zeng YJ, et al. (2006) ZnO light-emitting diode grown by plasma-assisted metal organic chemical vapor deposition. *Appl Phys Lett* 88: 173506.
22. Zheng K, Guo Q, Wang EG (2008) A buffer layer for ZnO film growth on sapphire. *Surf Sci* 602: 2600–2603.
23. Boschloo G, Hagfeldt A (2009) Characteristics of the iodide/triiodide redox mediator in dye-sensitized solar cells. *Acc Chem Res* 42: 1819–1826.
24. Kato N, Takeda Y, Higuchi K, et al. (2009) Degradation analysis of dye-sensitized solar cell module after long-term stability test under outdoor working condition. *Sol Energy Mat Sol C* 93: 893–897.
25. Grätzel M (2006) Photovoltaic performance and long-term stability of dye-sensitized mesoscopic solar cells. *C R Chim* 9: 578–583.
26. Elumalai NK, Uddin A (2016) Open circuit voltage of organic solar cells: An in-depth review. *Energy Environ Sci* 9: 391–410.



**AIMS Press**

© 2018 the Author(s), licensee AIMS Press. This is an open access article distributed under the terms of the Creative Commons Attribution License (<http://creativecommons.org/licenses/by/4.0>)